Cartilage Tissue Engineering Using Electrospun PCL Nanofiber Meshes and MSCs

M. L. Alves da Silva,*,†,‡ A. Martins,†,‡ A. R. Costa-Pinto,†,‡ P. Costa,†,‡ S. Faria,§ M. Gomes,†,‡ R. L. Reis,†,‡ and N. M. Neves†,‡

3B's Research Group—Biomaterials, Biodegradables and Biomimetics, University of Minho, Headquarters of the European Institute of Excellence on Tissue Engineering and Regenerative Medicine, AvePark, Zona Industrial da Gandra, S. Claudio do Barco, 4806-909 Caldas das Taipas, Guimarães, Portugal, IBB—Institute for Biotechnology and Bioengineering, PT Associated Laboratory, Guimarães, Portugal, and CMAT—Mathematical Research Centre, Department of Mathematics and Applications, University of Minho, Campus de Azurém, 4800-058, Guimarães, Portugal

Received May 3, 2010; Revised Manuscript Received September 12, 2010

Mesenchymal stem cells (MSCs) have been recognized for their ability to differentiate into cells of different tissues such as bone, cartilage, or adipose tissue, and therefore are of great interest for potential therapeutic strategies. Adherent, colony-forming, fibroblastic cells were isolated from human bone marrow aspirates, from patients undergoing knee arthroplasties, and the MSCs phenotype characterized by flow cytometry. Afterward, cells were seeded onto electrospun polycaprolactone nanofiber meshes and cultured in a multichamber flow perfusion bioreactor to determine their ability to produce cartilagineous extracellular matrix. Results indicate that the flow perfusion bioreactor increased the chondrogenic differentiation of hBM-MSCs, as confirmed either by morphological and RT-PCR analysis. Cartilage-related genes such as aggrecan, collagen type II, and Sox9 were expressed. ECM deposition was also detected by histological procedures. Collagen type II was present in the samples, as well as collagen type I. Despite no statistically significant values being obtained for gene expression, the other results support the choice of the bioreactor for this type of culture.

Introduction

Due to the epidemiological importance and the high social costs of joint diseases, cartilage engineering holds remarkable potential in orthopedic surgery as an alternative to current surgical methods. Traditional implantable materials frequently fail its biofunction, due to implant loosening, inflammation, infection, rejection, wear debris, and tissue inflammation or infection.[1] Tissue engineering (TE) can provide the answers to many of these problems. One of the challenges of TE is to mimic the natural extracellular matrix (ECM) of connective tissues, including cartilage. Nanoscale is very important in this approach, as the ECM substratum that interacts with cells includes fibrils at submicrometer level.[2] The electrospinning process has been used to produce nanofibrous scaffolds that can mimic a tissue's ECM by imitating its fibrils morphology and distribution.[3] These nanofibrous structures present many advantages, such as high specific surface area for cell attachment, higher microporous structure and a 3D microenvironment for cell−cell and cell-biomaterial contact.[1,4] In the past few years, nanomaterials and nanofibers have been explored as new functional structures for tissue regeneration in bone,[5] cartilage,[6] veins, or nerves.[7] Some materials intended for cartilage TE have been produced using electrospinning of several synthetic and natural materials, such as PCL,[8] PLGA,[9] chitosan-based materials,[10] or starch-based materials.[11]

Cartilage is an avascular tissue composed of chondrocytes entrapped in an ECM rich in proteoglycans and collagens.[12] The low self-regeneration potential of cartilage is due to the absence of vascular networks and progenitor cells in the tissue, as well as the nonmobility of chondrocytes in the dense ECM.[13] Chondrocytes have been used to generate engineered cartilage tissue,[11,14] and are usually isolated from articular cartilage tissues. Stem cells are also commonly proposed for cartilage TE. Chondrocytes are developmentally derived from stem cells.[15] Compared with adult chondrocytes, stem cells are easier to obtain and manipulate, as they can undergo several passages before loosening their differentiation potential.[16] Mesenchymal stem cells (MSCs) can be isolated from several tissues, including bone marrow,[17] fat tissue,[18] or synovium.[19] Selecting the ideal source of cells for a cartilage TE approach is a demanding and challenging task, as there are numerous options. Additionally, the choice of the scaffold is very important. A recent study showed dissimilar chondrogenic differentiation behavior of MSCs derived from different tissues, namely, human embryonic stem cells, bone marrow, and adipose tissue. Additionally, their behavior also differs among the tested silk and chitosan scaffolds.[16]

Dynamic culture systems or bioreactors have been widely studied for cartilage TE approaches.[20−22] Results often show that they enhance ECM formation when compared with static cultures. In some bioreactor studies for cartilage TE approaches, low levels of shear stress were used successfully, as they promoted good mass transfer properties.[23] As chondrocytes are surrounded by an environment influenced by mechanical forces, it is logical that the formation of cartilagineous tissue is also heavily influenced by the environment. Therefore, if cells are surrounded by an appropriated environment and they have access to the correct levels of nutrients, it is believed that they will act like native chondrocytes and secrete ECM.[23]

* Corresponding author: msilva@dep.uminho.pt.
† 3B's Research Group.
‡ IBB.
§ CMAT.

10.1021/bm100476r
Published on Web 11/24/2010

In a recent work using a bovine articular chondrocytes model, we showed that polycaprolactone (PCL) and SPCL (starch-compounded PCL) nanofiber meshes are suitable for cartilage TE.[11] In that study, we used a high initial concentration of bovine articular chondrocytes and cultured the nanofiber meshes in a lab rotator bioreactor. The results were encouraging, but from that work, several other questions were raised, namely, the aspects involved in the future application of this model in human therapies. In that study a high number of cells were used, which most of the time are not readily available for clinical application. The dynamic culture system used in that previous study did not allow the creation of a controlled environment for the culture of the constructs, and it is important to obtain a preimplant with similar characteristics to the native cartilage. Finally, when going to the clinic, the access to articular chondrocytes is more limited than it is for MSCs. Having all these issues in mind, we designed this study to validate if, starting from low seeding densities of human bone marrow-derived MSCs in PCL nanofiber meshes cultured in an in-house developed multichamber flow perfusion bioreactor (PT Patent No. 104155; European patent pending[24]), we could induce chondrogenic differentiation of the MSCs and consequent ECM deposition. Also, we aimed to determine whether the ECM deposition would result in cartilage-like tissue, whose characteristics would resemble native articular cartilage.

Materials and Methods

1. Nanofiber Meshes Processing. A polymeric solution of PCL (PCL 787, TONE polymer, Union Carbide Chemical and Plastics Division, Bound Brook, NJ, with 80 kDa), at the concentration of 17% (w/v), was prepared by dissolving the polymer into an organic solvent mixture of chloroform/dimethylformamide (70:30; Sigma-Aldrich, U.S.A.). The polymeric solution was placed into a syringe, which is coupled to a syringe pump (model KDS100, KD Scientific, U.S.A.) for flow rate control. A blunted metallic needle with an internal diameter of 0.8 mm was attached to the syringe. A grounded aluminum foil was used as the fiber mesh collector. A high voltage of 9 kV was applied to the needle tip to generate the electric field; a needle tip-to-collector distance of 20 cm and the flow rate of 1.0 mL/h were established. The applied voltage was maintained at 9 kV. All the experiments were performed at room temperature and the conditions were optimized for the production of PCL nanofiber meshes. The produced PCL nanofiber meshes presented a thickness between 40−60 μm, 70−80% of porosity, determined by nCT (data not shown) and an average pore size of 2.7 μm. For more details on the PCL nanofiber meshes, please refer to Guimarães et al., 2010.[25] After collection, nanofiber meshes were cut into 1 cm^2 squares.

A clamping system to fixate the produced nanofiber meshes in the multichamber flow perfusion bioreactor (PT Patent No. 104155; European patent pending[24]) had to be assembled. The meshes were fixated in between two silicon rings, which were then clamped with nylon stitches.[25] Using this clamping system, the available surface of the nanofiber meshes to be cultured in the bioreactor was a circle of 5 mm in diameter. For the static cultures, the referred 1 cm^2 squares were used. The membranes were then sterilized under UV light for 1 h on each side.

2. Isolation of hBM-MSCs. hBM-MSCs were isolated from bone-marrow aspirates collected under informed consent from patients undergoing knee arthroplasties in Hospital de S. Marcos, Braga, Portugal. Samples were collected from a 55 year old female donor, isolated, expanded, and frozen in several passages. Briefly, during the surgery, bone marrow was collected to a container with α-MEM medium (Invitrogen/12000−063), supplemented with antibiotic/antimycotic solution (Gibco/15240062) and 5000 units of heparin (Sigma/H3393) and maintained in ice until the isolation procedure. Aspirates were homogenized, diluted in PBS (Sigma/P4417; 1:1), and incubated for 5 min at room temperature. Then, bone marrow was diluted in lyses buffer (1:10) and left under agitation for 10 min. Lyses buffer was prepared with 10 mM of Tris-HCl (Sigma/T3253), 1.21 g of Tris Base (Sigma/T1503), and 8.3 g of NH_4Cl (Merck/1011455000) in 1 L of distilled water. Afterward, the suspension was centrifuged at 1200 rpm for 15 min at room temperature. Cells were resuspended in α-MEM medium, supplemented with antibiotic/antimycotic solution and 20% FBS (Biochrom/BSC0115/0943k). Cell suspension was filtered for disposal of debris, using 100 and 70 μm Cell Strainer (BD Falcon/352360 and BD Falcon/352350). Cells were counted and plated at a density of 4.7×10^3 cells/cm^2. Cells were expanded in the referred culture medium until passage 5 and then used for seeding the nanofiber meshes.

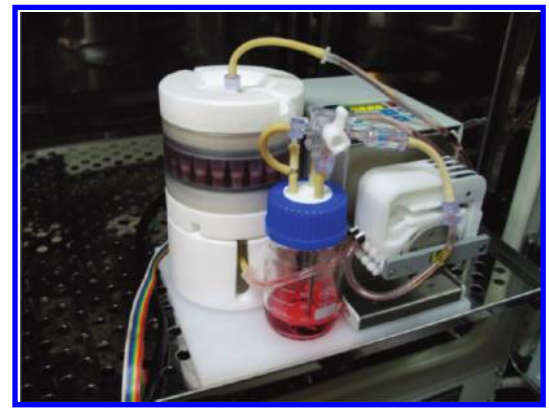

Figure 1. Multichamber flow perfusion bioreactor (PT Patent No. 104155; European patent pending[24]) assembled and the culture system inside the incubator.

3. Flow-Cytometry Analysis. To evaluate cell-surface marker expression, cultured cells were incubated for 20 min at 4 °C with fluorescein isothiocyanate (FITC)- or phycoerythrin (PE)-conjugated monoclonal antibodies specific for human markers associated with mesenchymal and hematopoietic lineages. The antibodies used were CD29, CD34, CD45, CD73, CD90, CD105, and CD116. All the antibodies were purchased from BD Pharmingen. The samples were analyzed on a FACS Calibur (BD Biosciences).

4. hBM-MSCs Culture on the Multichamber Flow Perfusion Bioreactor. hBM-MSCs were detached from the culture flasks by treatment with trypsin/EDTA solution (Invitrogen/25300-062). Cells were counted and a cell suspension of 200.000 cells/nanofiber mesh was prepared to seed each of the nanofiber meshes. Cell seeding was performed using the "drop" method. The seeding method has been described previously in more detail by our group, in Guimarães et al., 2010.[25] Briefly, each scaffold was seeded with a 10 μL drop of α-MEM culture medium containing 200.000 cells, in 24-well plates. Afterward, the constructs were maintained at 37 °C and 5% CO_2, during 4 h in an incubator to allow cell attachment to the scaffolds. After this time period, culture medium was added to each culture well and left in the incubator for 24 h. The constructs were then transferred to the bioreactor.

This is the first work reporting the use of the multichamber bioreactor designed by our group. The bioreactor has currently a PT patent, and the European patent is under submission. For detailed information, please refer to Costa et al., 2010.[24] Briefly, the bioreactor apparatus is composed of a central part with 20 individual culture chambers, with a diameter of 8 mm each, and two lids attached to the central part. These lids form a common inlet and outlet of medium. These chambers were designed in a way that allows the circulation of the culture medium through them and assures the even distribution of it between the several flow chambers. For bioreactor cultures, 20 constructs were transferred for the apparatus and placed one in each chamber. A flow velocity of 70 μL/min/nanofiber mesh was established. The bioreactor apparatus herein used can be observed in Figure 1. The clamping system has been previously reported also by a work in our group by Guimarães et al., 2010.[25]

Another set of 20 constructs was transferred to new culture plates and maintained in static conditions to be used as control. Chondrogenic differentiation medium consisting of α-MEM supplemented with antibiotic/antimycotic solution, ITS liquid media supplement (Sigma/I2521), dexamethasone 1 mM (Sigma/D1756), sodium pyruvate 0.1 M (Sigma/P4562), ascorbate-2-phosphate 17 mM (Sigma/A4544), L-proline 35 mM (Sigma/P5607), and 1 ng/mL of human recombinant TGF-β3 (PeproTech/100-36) was used for the 28 days of the experiment. Culture medium in the bioreactor was completely changed every week (100 mL each time). Control samples were cultured in 24-well plates and were fed every other day with 1 mL of culture medium.

Samples were collected at every time point, both from the bioreactor and from static controls. For DNA analysis, two samples were collected at 14, 21, and 28 days of the experiment. For SEM analysis, 1 sample was collected on every time point. Three samples at 14, 21, and 28 days were collected for PCR analysis. For histological procedures, one sample was collected at the end of the experiment. Experiments were repeated three times.

5. Proliferation Assay (DNA Quantification). Evaluation of cell proliferation was performed using the PicoGreen dsDNA quantification Kit (Molecular Probes/P-7589), according to the manufacturer instructions. Samples from the flow perfusion bioreactor and from the static control were collected at 14, 21, and 28 days. Triplicates of every time point were used. A standard curve ranging from 0.0 to 1.5 μg/mL was established. Fluorescence of both samples and standard curve was read with an excitation of 485/20 nm and an emission of 528/20 nm. DNA concentration was extrapolated from the standard curve.

6. Scanning Electron Microscopy (SEM). For SEM analysis, one hMSCS-nanofiber mesh construct was collected at each time point: 1, 2, 3, and 4 weeks, for each culture condition. They were washed in sterile PBS and immersed in 3% glutaraldehyde (Sigma/G-5882) at room temperature for 1 h. Samples were washed in PBS, dehydrated in increasing ethanol concentrations, and let to dry at room temperature. Samples were sputter coated with gold and analyzed in a scanning electron microscope (Model S360, Leica Cambridge, U.K.).

7. RNA Isolation. Three samples were collected from the flow perfusion bioreactor and from the static control. Samples were washed in PBS, immersed in TRIzol reagent (Invitrogen/15596−018) and kept at −80 °C for posterior RNA extraction. To perform the RNA extraction, samples were taken from the freezer and kept in ice until complete thawing. Chloroform (Sigma/C-2432) was added; samples were vigorously agitated for 15 s and then incubated in ice for 15 min. After that incubation, samples were centrifuged at 13000 rpm, for 15 min, at 4 °C. Afterward, the supernatant was collected for a sterile 1.5 mL tube, and an equivalent volume of isopropanol (Sigma/I-9516) was added. Samples were incubated at −20 °C overnight to precipitate the RNA. In the next day, samples were centrifuged at 13000 rpm, for 15 min, at 4 °C. Then, the supernatant was removed and 800 μL of ethanol 70% was added to wash away the isopropanol. The ethanol 70% solution was prepared from absolute ethanol (Merck/1.00983.2511) and ultrapure water. The 1.5 mL tubes were agitated vigorously and centrifuged again, at 9000 rpm for 5 min, at 4 °C. The supernatant was again removed, and the pellet was left to air-dry. Finally, the pellet was resuspended in 50 μL of DNase, RNase free water (Gibco/10977-015). The concentration and purity of the extracted RNA was evaluated using the NanoDrop ND-1000 Spectrophotometer (NanoDrop Technologies Inc., U.S.A.).

8. Real Time PCR. The real time PCR procedure used in the present work consisted of a two-step fluorogenic assay using the SyberGreen system (Bio-Rad). All the reagents used in this procedure were from Bio-Rad, following the instructions of the manufacturer. Thermocycler reaction conditions used were also the mentioned in the kits. In the first step, RNA was reverse transcribed into cDNA using the iScript cDNA synthesis kit (1708891). A MiniOpticon real-time PCR detection system (BioRad Laboratories, U.S.A.) was used to perform the reaction. Afterward, the cDNA obtained was used as template for the amplification of the target genes (aggrecan, collagen type I, II, and X, Sox9 and Runx2), with the Syber Green Kit (1708884). The number of amplification cycles used for every reaction was of 45. GAPDH was used as reference gene, and the expression of all the target genes was normalized to the GAPDH expression of that sample. All the primer sequences were generated using Primer3 software[26] and acquired from MWG Biotech AG, Germany. Primers sequences used are shown in Table 1. Obtained results were analyzed with CFX Manager Software, version 1.5 (BioRad Laboratories, U.S.A.).

Table 1. Primer Sequences Used for RT-PCR Procedures[a]

gene	forward (5′−3′)	reverse (5′−3′)
AGC	TGAGTCCTCAAGCCTCCTGT	TGGTCTGCAGCAGTTGATTC
COL II	CGGTGAGAAGGGAGAAGTTG	GACCGGTCACTCCAGTAGGA
COL I	AGCCAGCAGATCGAGAACAT	ACACAGGTCTCACCGGTTTC
COL X	CCAGGTCTCGATGGTCCTAA	GTCCTCCAACTCCAGGATCA
Runx2	TTCCAGACCAGCAGCACTC	CAGCGTCAACACCATCATTC
Sox9	TTCATGAAGATGACCGACGC	GTCCAGTCGTAGCCCTTGAG
GAPDH	ACAGTCAGCCGCATCTTCTT	ACGACCAAATCCGTTGACTC

[a] AGC = Agreccan; COL II = collagen type II; COL I = collagen type I; COL X = collagen type X; Runx2 = runt-related transcription factor 2; Sox9 = Sry-type high mobility group box 9; GAPDH = glyceraldehyde 3-phosphate dehydrogenase.

8. Histological Analysis. Samples were collected at the end of the experiment, included in OCT (Gurr/OCT compound/BDH) and stored at −20 °C. Sections with 8 μm thickness were placed in microscopy slides, fixed in a fresh 4% paraformaldehyde (PF) (Sigma/P-6148) solution in PBS buffer, during 30 min at 4 °C, washed twice in distilled water, and left overnight to air-dry. Slides were stored at 4 °C until they were further used for staining procedures. Toluidine blue staining was performed. Staining solution was prepared by adding 1% of toluidine blue (Sigma/T-0394) dissolved in distilled water containing 0.5 g of sodium borate, followed by filtering. One drop of this solution was added to each section for 2−3 s. Then, the sections were rinsed with distilled water and allowed to air-dry overnight. Sections were cleared in a xylene substitute (Sigma/A5597) and mounted in Histo clear (Frilabo/HS200). Safranin O staining was performed by washing slides in tap water, then immersed in 0.02% fast green (Fluka/44715) for 3 min. Then, samples were immersed in 1% acetic acid (Panreac/131008) solution for 30 s. After, slides were immersed in 0.1% safranin O (Fluka/84120) solution for 5 min. By the end, slides were washed in tap water and allowed to air-dry. Sections were cleared in xylene and mounted as previously described.

10. Immunolocalization of Type I and II Collagens. Immunolocalization of type I and type II collagens was performed in fixed sections. Endogenous peroxidase activity was quenched with 0.3% hydrogen peroxide solution for 30 min. Sections were rinsed in PBS for 5 min. RTU Vectastain Universal Elite ABC Kit (Vector/VCPK-7200) was used for antibody incubation according to the instructions of the manufacturer. Shortly, sections were incubated with primary antibodies (collagen type I and collagen type II; UNLB/Goat antitype I collagen 1310-01 and UNLB/Goat antitype II collagen 1320-01) overnight at 4 °C, in a humidified atmosphere. Incubation was revealed by using the Peroxidase Substrate Kit DAB (Vector/VCSK-4100). Slides were washed in water for 5 min and then counterstained with hematoxylin for nuclei visualization. Finally, slides were mounted in Histo clear. Controls were performed using normal goat serum instead of primary antibodies, which was also included in the kit.

11. Statistical Analysis. Statistical analysis was performed using the SPSS statistic software (Release 15.0.0 for Windows). First, a Shapiro−Wilk test was used to ascertain the data normality and variance equality. The normality is strongly rejected and, consequently, nonparametric tests were used in further comparisons between static and dynamic culture conditions. A Mann−Whitney U-test was applied to compare the two independent groups of samples for each variable (i.e., DNA quantification and real-time PCR). P values lower than 0.01 were considered statistically significant in the analysis of the results. A Kruskal−Wallis test was applied to compare differences in between the days in each group. P values lower than 0.01 were considered statistically significant in the analysis of the results.

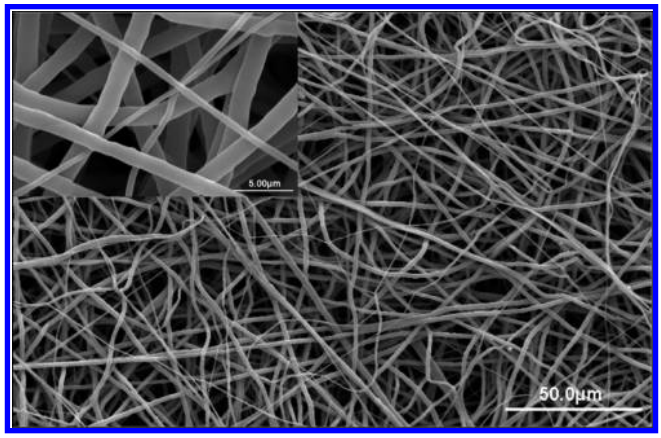

Figure 2. SEM micrographs of poly(ε-caprolactone) (PCL) nanofiber meshes processed by electrospinning. Scale bars: 50.0 μm = 5 cm; 5.0 μm = 2 cm.

Results

1. Electrospun PCL Nanofiber Meshes. SEM observations of the produced nanofiber meshes show a random distribution as expected. This is the most typical morphology obtained in the electrospinning process, caused by the electric field generated in the equipment (Figure 2). PCL nanofiber meshes were composed by nanofibers with diameters in the submicrometer range, from 0.4 to 1.4 μm.

2. FCM Analysis of the Isolated Cells. Isolated bone marrow cells were expanded and characterized for specific surface antigen expression by flow cytometry analysis. hBM-MSCs were analyzed for hematopoietic marker expression (CD34 and CD45): isolated cells were negative for these two markers (not detected, less than 5%). Cells were positive for CD29 (95%), CD73 (98.3%), CD90 (97.9%), CD105 (85%), and CD166 (85%) surface markers, which are characteristic of mesenchymal stem cells. Based in this data we are very confident that the cell fraction isolated from bone marrow contains mostly MSCs.

3. DNA Quantification. Results show a higher DNA content in samples collected from the flow perfusion bioreactor, compared to the static control conditions, in terms of DNA concentration (Figure 3). In this condition, DNA contents decreased a little at 21 days, but then increased by 28 days. In static conditions samples, there is a continuous decrease of the DNA contents along the time. To find significant differences in DNA contents between static and bioreactor culture conditions, the Mann−Whitney U-test was performed. No significant differences between both culture conditions were found at 14 ($p = 0.18$) or 21 days of experiment ($p = 1.00$). However, bioreactor samples displayed a significantly higher DNA quantification than the static ones at 28 days of experiment ($p = 0.002$).

Concerning statistic differences between the days of culture, we found none either in static (Kruskal−Wallis test, $p = 0.149$) or in the bioreactor (Kruskal−Wallis test, $p = 0.261$).

4. SEM Analysis. SEM observations of the cultured hBM-MSC in electrospun PCL nanofiber meshes shows some differences in their morphology along the experiment (Figure 4). At 7 days of culture, samples from the bioreactor showed a round-shaped morphology, whereas the cells from the static culture samples presented a fibroblast-like morphology, very stretched. The round-shaped morphology of cells in the bioreactor samples is maintained throughout the time course of the experiment (Figure 4A,C,E,G). In the two last time points, the cells morphology is not that evident. In Figure 4E and G, referring to the bioreactor cultures at days 21 and 28, respectively, we can observe that cells form a sheet that covers the entire mesh surface. Our interpretation of these two figures is that the production of ECM component and consequent deposition led to a thin film of cells entrapped in this matrix. Therefore, there are less "visible" cells, as they are now part of the matrix. On the other hand, in static cultures we can observe individual cells, as the matrix production here seems to be delayed, in comparison to the bioreactor cultures. Cells in static samples seem to be acquiring the round-shaped morphology along the time, but by the 28th day of culture they are still not as round-shaped as the bioreactor (Figure 4G,H).

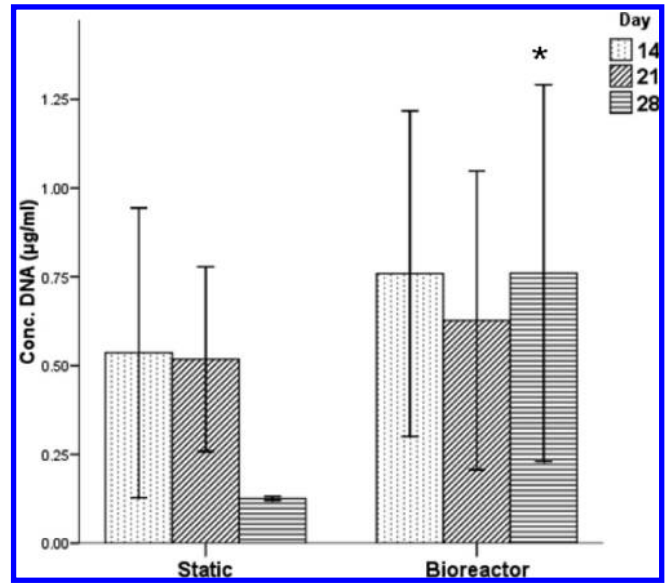

Figure 3. Box plot of the DNA quantification in static and bioreactor cultures after 14, 21, and 28 days of culture. Data were analyzed by the nonparametric way of a Mann−Whitney U-test (*$p < 0.01$, vs Static).

5. Real-Time PCR. Samples were collected for real-time PCR at 14, 21, and 28 days of experiment, both from the bioreactor and static control culture conditions. The aim was to determine the expression of several cartilage-related genes. All the tested genes were being expressed. The expression of the *Aggrecan* transcript was detected for both culture conditions, in all time points. The statistical analysis performed, using a Mann−Whitney U-test, confirmed the absence of significant difference between culture conditions at 14 ($p = 1.000$), 21 ($p = 0.762$), and 28 days of experiment ($p = 0.800$; Figure 5). The collagen type II expression was detected, but no significant difference was found between static and bioreactor culture conditions on the 14th ($p = 0.233$), 21st ($p = 0.413$), and 28th day of experiment ($p = 0.400$). The *Sox9* transcript is observed in both culture conditions, following a similar expression pattern. Statistical analysis of the results for 14 ($p = 1.000$), 21 ($p = 0.800$), and 28 days of culture ($p = 0.333$) showed no significant difference between both culture conditions. The expression of collagen type I showed no significant difference between bioreactor and static culture conditions found in the 14th ($p = 0.563$), 21st day ($p = 0.075$), or 28th day ($p = 0.071$). Collagen type X is expressed in slightly equal values for both types of cultures, as well as *Runx2*. Statistical analysis for collagen type X confirmed that no significant difference was found between culture conditions in the 14th ($p = 1$), 21st ($p = 0.4$), or 28th day ($p = 1$). For *Runx2*, the same was observed: no significant difference between the two tested conditions was found in the 21st ($p = 0.400$) or in the 28th day of experiment ($p = 1.00$).

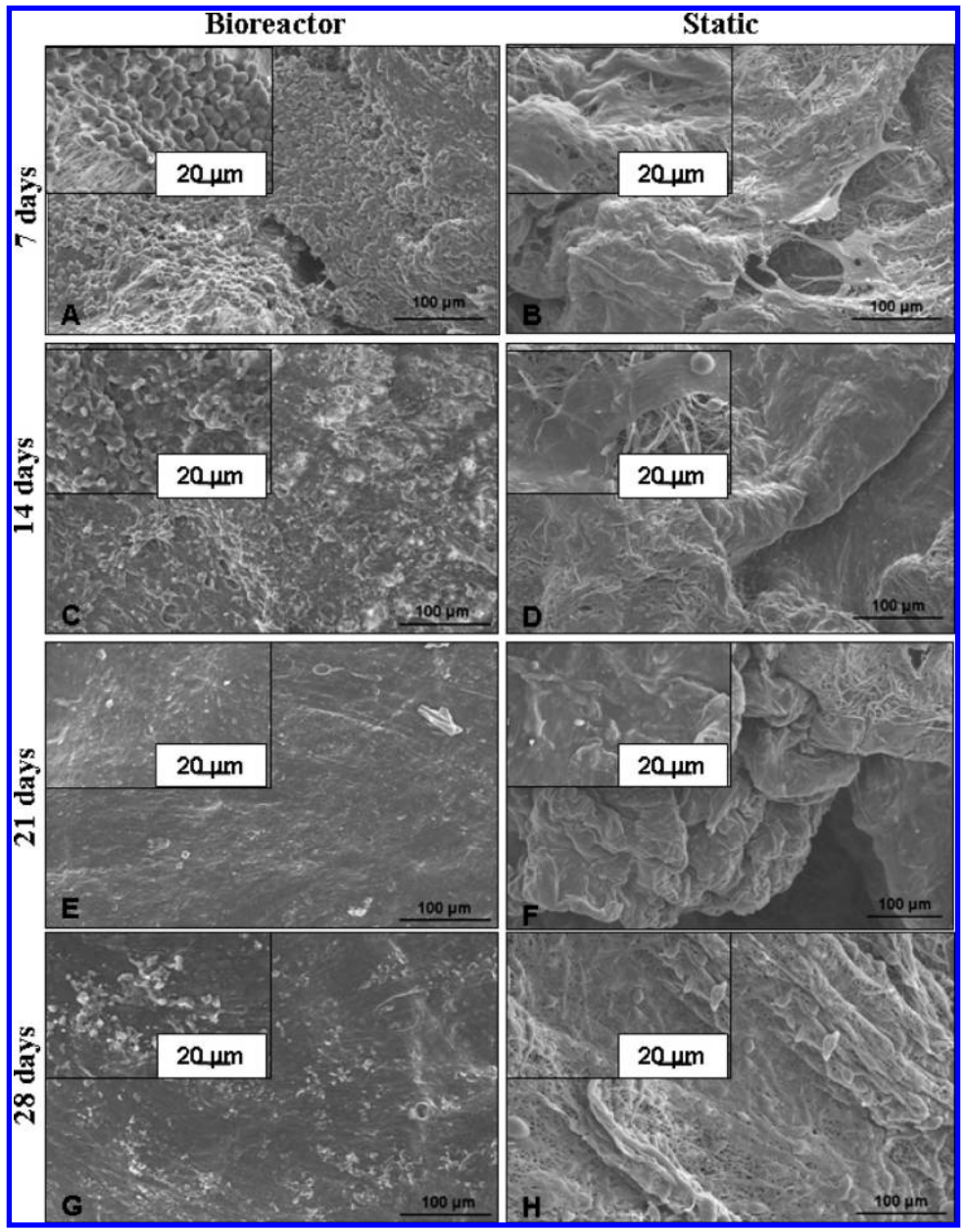

Figure 4. Morphology of hBM-MSCs cultured in electrospun PCL nanofiber meshes, in the flow perfusion bioreactor (A, C, E, G) and in static control conditions (B, D, F, H) along the time course of the experiment: (A, B) 7 days; (C, D) 14 days; (E, F) 21 days; and (G, H) 28 days. Different magnifications were used to highlight cell morphology. Scale bars: 100 μm = 2 cm; 20 μm = 0.5 cm.

6. Histological Staining. Histological sections of electrospun PCL nanofiber meshes seeded and cultured with hBMSCs, at 28 days of culture in the multichamber bioreactor or in static conditions were stained for cartilagineous ECM using toluidine blue and safranin O assays (Figure 6). Toluidine blue staining detected the presence of glycosaminoglycans in those sections, and safranin O staining confirmed this observation. It is also possible to observe a dense concentration of staining on sections from the bioreactor samples (Figure 6A,B) compared to the static culture sections on both toluidine blue and safranin O staining.

7. Immunolocalization of Collagen Types I and II. Histological sections of electrospun PCL nanofiber meshes cultured with hBMSCs at 28 days of culture in the multichamber bioreactor or in static conditions were stained for immunolocalization of collagen types I and II (Figure 7). For the bioreactor cultures, both types of collagens were detected. Collagen type I stain (Figure 7A) appears to be slightly more clear than the collagen type II staining (Figure 7B). On the other hand, there is a heavy unspecific staining on the control sections of both types of cultures (Figure 7A,D), which may have in part been due to dye trapped in folded regions of the sections. In static cultures, a marked staining for collagen type I (Figure 7E) can be observed, when compared to the collagen type II section (Figure 7F).

Discussion

Bioreactors are a powerful tool in several areas of TE. In cartilage TE, they can provide mechanical stimulus to cells, as well as better access of nutrients, enhancing the production of ECM. In the present work, we aimed to study the effect of a new multichamber flow perfusion bioreactor in the chondrogenic differentiation of hBM-MSCs when seeded onto electrospun PCL nanofiber meshes. The present work is one of the first reports that we release concerning the utilization of the multichamber bioreactor and the present data is starting point

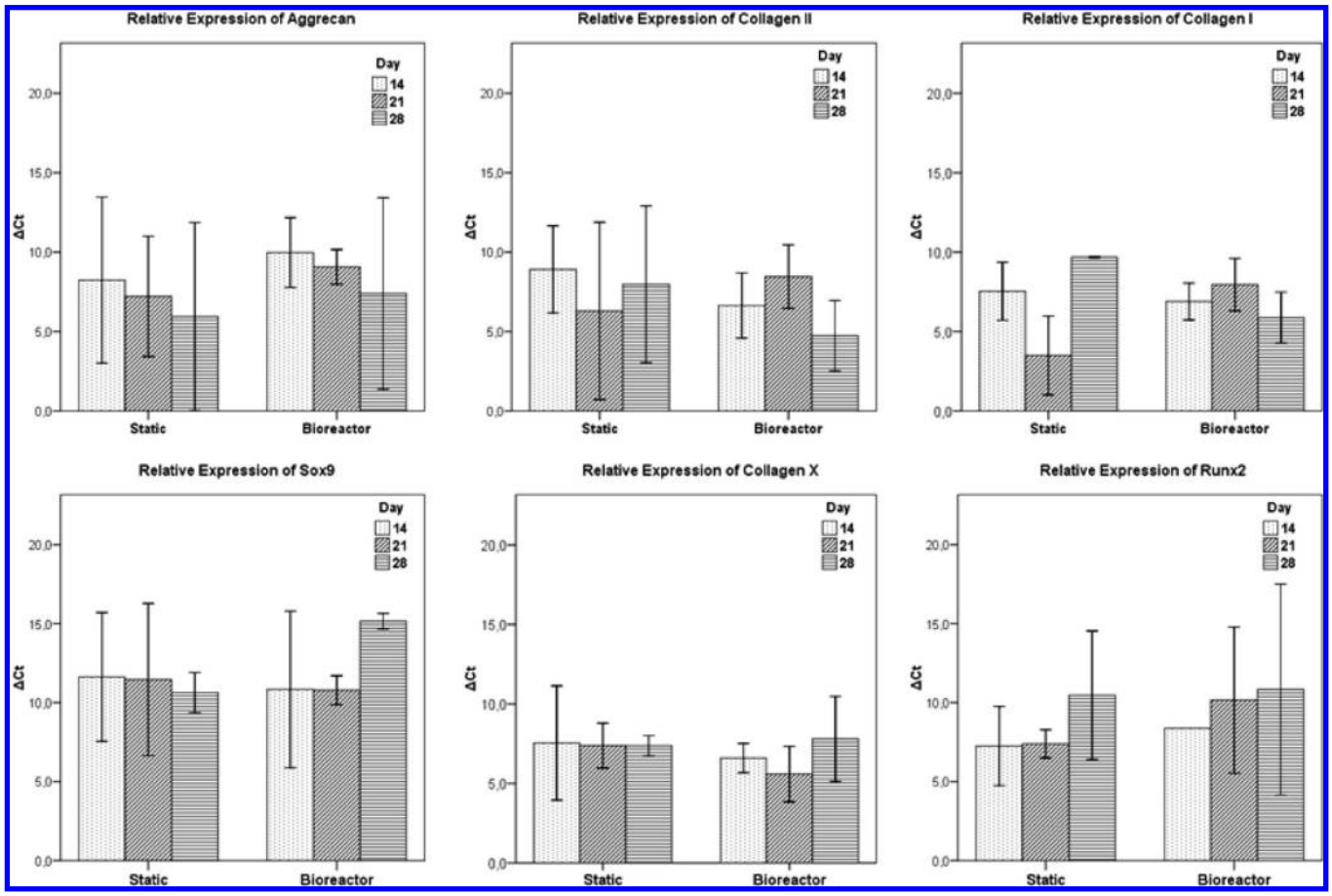

Figure 5. Bar plots of chondrogenic markers of flow perfusion bioreactor samples and static control conditions normalized for the reference gene GAPDH, after 14, 21, and 28 days of culture. Data were analyzed with a Mann−Whitney U-test.

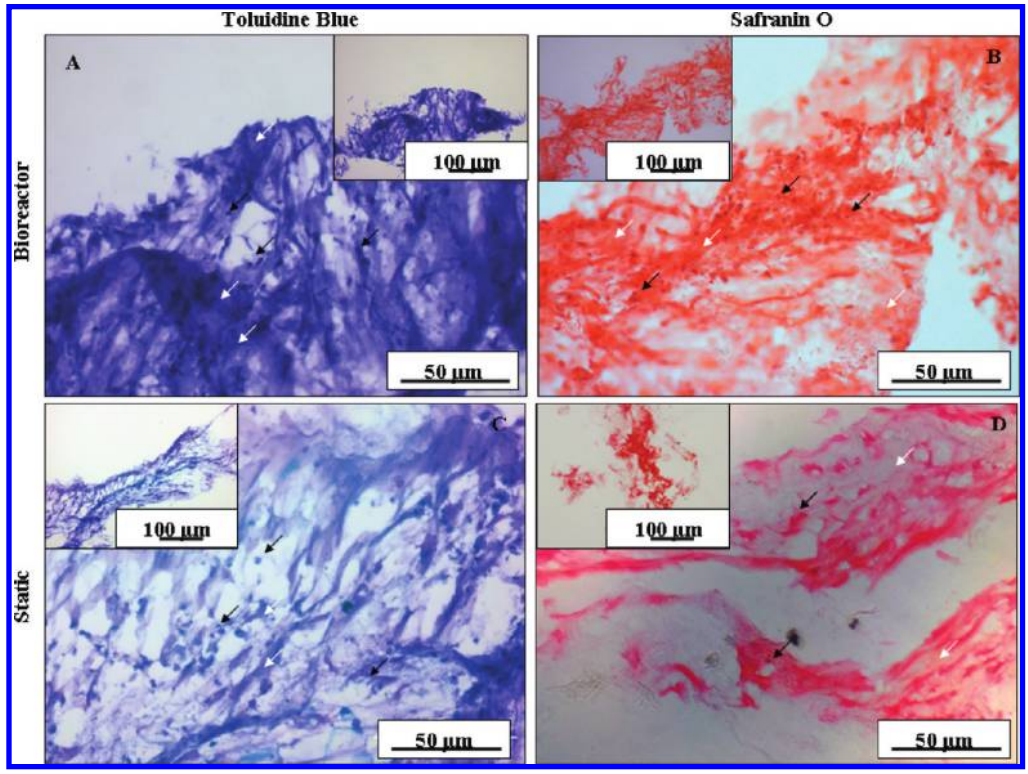

Figure 6. - Histological section of hBMSCs seeded onto PCL nanofiber meshes for chondrogenic differentiation, at 28 days, from bioreactor constructs (A, B) and static control cultures (C, D): (A, C) toluidine blue staining; (B, D) safranin O staining. Black arrows show the nuclei of the cells. White arrows show ECM. Scale bars: 100 μm = 1 cm; 50 μm = 2.5 cm.

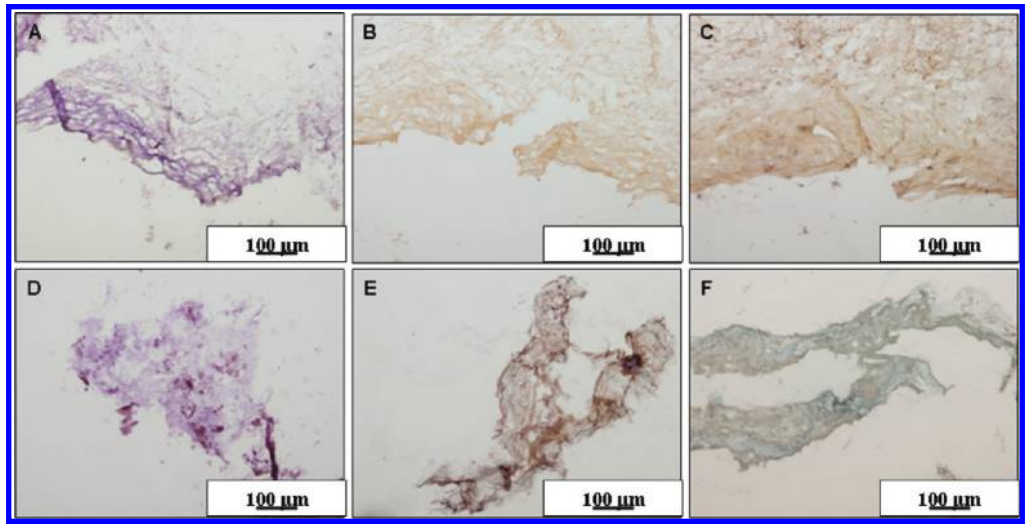

Figure 7. Immunolocalization of collagen type I (B, E) and type II (C, F) in electrospun PCL nanofiber meshes, after 28 days of culture in the bioreactor (A−C) and in static cultures (D−F). Controls of the immunohistochemistry assay (A) were performed with normal horse serum. Scale bar: 100 μm = 1 cm.

for optimization of the culture conditions used, as several new questions were raised from the obtained results. It has been demonstrated that the quality of tissue-engineered cartilage can be manipulated depending on the type and seeding density of cells and bioreactor culture conditions.[27] Several perfusion bioreactors have been developed in recent years, aiming to enhance tissue growth in in vitro constructs,[27−29] for example, for bone,[30] dermal tissues,[31] and cartilage.[32] Dynamic flow conditions are known to enhance cartilage development compared to static cultures.[32−36] For detailed review please refer to Godara et al., 2008 and Butler et al., 2009.[37,38] Fluid flow enhances nutrient and waste exchange in vitro, improving mass transport and delivering shear stress within the construct.[39] In perfusion bioreactors, the level of shear stress and of nutrient transfer can be easily changed by modifying the medium flow rate, and thus, the quality of the tissue engineered construct can be improved, depending on the media flow velocity.[33] In the present work, we used a media flow of 70 μL/min/nanofiber mesh. We based our choice of the flow velocity in the literature. However, references using nanofiber meshes are scarce, if not inexistent. Reported flow velocity for 3-D constructs for cartilage TE range from 0.01 to 5 mL/min.[27,28,39,40] We decided to choose a low flow velocity as a starting point to allow the deposition of the ECM components. As we performed a low density seeding, the chosen perfusion velocity would allow, in our perspective, to provide cells the nutrients and oxygen needed. We would expect cell proliferation, differentiation and consequent enhanced deposition of ECM components along the time. As for cell numbers, the amount of cellular DNA varied along the experiment, being observed a high decrease in static culture conditions at the 28th day. In this time point, bioreactor samples displayed a significantly higher DNA quantification than static ($p = 0.002$). It is the fair to state that, in terms of cell proliferation, the chosen fluid flow was beneficial for the constructs cultured in the bioreactor, enhancing cell proliferation. The beneficial effect of directional fluid flow has been demonstrated by Tarng and co-workers, using periosteal explants secured onto PCL scaffolds and cultured in spinner flasks. The authors showed that fluid flow enhanced cell proliferation, chondrogenic differentiation and cell organization.[41]

Morphological observation of cells showed some differences between the two conditions. Cells in the bioreactor samples have acquired a round-shaped morphology at early stages of culture (i.e., 7th and 14th day), whereas the cells cultured in static conditions are stretched and flat until at least the 21st day of culture. These observations may be related to the fluid flow in the bioreactor samples. The beneficial effect of the perfusion can be observed, as the chondrogenic morphology seems to be highlighted in these samples, whereas in the static ones, the morphology change can be observed only after 21 days in culture. TGF-β3 is the essential growth factor for promoting chondrogenesis both in vivo and in vitro conditions.[42] It has been shown that TGF-β3 induced hBMSCs having increased *Sox9* expression with the presence of collagen type II and aggrecan.[43] Although the cartilage obtained in this study showed some signs of hypertrophy, induced either by the flow perfusion or by the utilization of TGF-β3, the conjugation of both factors may have contributed for the increased chondrogenesis at the early stages of culture, for the bioreactor samples. Chondrogenesis at early stages of cultures have been also observed when culturing chitosan-BMP6 loaded scaffolds with ATDC5 chondrocytes cell line in RCMW reactors.[44] Additionally, cells cultured in static cultures showed hypertrophy, contrarily to the observed in the cultures from the bioreactor. This is not the case of our results, as the presence of hypertrophy related genes was detected in both static and dynamic cultures. Hypertrophy was also observed by Jung and coauthors, when they applied continuous compressive deformation for 10 or 24 days to PLCL scaffolds seeded with chondrocytes. These constructs were then implanted subcutaneously in nude mice. The observations showed hypertrophic forms in the implants stimulated for 24 days, demonstrating that the proper periodical application of dynamic compression can enhance GAGs production.[45]

No statistical differences were found between the expression levels in the bioreactor samples and the static control cultures. Cartilage-related genes expression such as aggrecan, collagen type II, and *Sox9*, was detected for both conditions. *Sox9* is highly expressed, stimulating the production of these genes. The high values obtained for standard deviations may be related to the flow velocity inside the fiber meshes. The dissimilar geometry of the scaffolds or of the flow perfusion may lead to different local shear stressed in each sample, even for the same input flow velocity.[39] Thus, the random morphology of the nanofiber meshes may be influencing the results within the same replicates. This fact, along with the common inlet and outlet of the bioreactor, could have resulted in nonuniform flow velocity

and therefore could have influenced the ECM deposition and generate the large standard deviations observed in the experiments.

hBM-MSCs cultured in the bioreactor were able to produce proteoglycans, as shown by the toluidine blue and safranin O staining. The presence of proteoglycans was also detected in the static samples. However, these sections revealed a less amount of staining when compared to the bioreactor sections. These stainings, together with the results of RT-PCR for the expression of aggrecan, indicate the deposition of ECM. Furthermore, collagen type I and type II present in both types of samples at 28 days was also detected by immunolocalization, which is consistent with the RT-PCR results. A different result was obtained by Li et al., 2008, using PLLA nanofibrous scaffolds cultured in a rotating wall vessel bioreactor for cartilage TE. Compared to the constructs obtained in static cultures, the bioreactor grown constructs produced more total collagen and GAGs and expressed higher levels of cartilage-related genes.[46]

The flow perfusion bioreactor used in this work provides a continuous flow of media through the construct, enhancing the mass transfer and the nutrients availability. However, the mechanical forces can have a detrimental effect in terms of damaging the neo-tissue formation.[40] In the present work, the bioreactor allowed the proliferation and chondrogenic differentiation of hBM-MSCs, but no significant differences were observed compared to the static cultures. Similar results were obtained for the chondrogenic differentiation of human adipose stem cells when cultured in PGA scaffolds using a recirculating bioreactor.[40] The authors showed that the chondrogenic differentiation, as well as the ECM formation, was not detrimentally affected by the bioreactor culture. The obtained results do not allow us to draw any conclusion concerning the enhanced effect of the bioreactor over chondrogenic differentiation of hBM-MSCs when seeded onto PCL nanofiber meshes. Some of the parameters of the experiment here reported have to be modified, for example, the number of initial cell seeding, nanofiber mesh structure, or even the fluid flow. We do sustain that this bioreactor is suitable for this type of culture, and further optimizations will be performed. The concept of nanofiber meshes cultured in bioreactors for cartilage TE has been proved to be applicable to this field, combined with efficient cell loading and bioreactor technology.[46]

Conclusions

Overall, we would like to highlight that the new flow perfusion bioreactor is suitable for culturing hBM-MSCs and electropun PCL nanofiber meshes. The culture in a flow perfusion bioreactor supported the attachment, proliferation, and chondrogenic differentiation of hBM-MSCs. The MSCs were able to produce ECM on the electrospun PCL nanofiber meshes, as stated by the staining and imunolocalization results. The media fluid flow may be influencing these results as well as the nanofiber mesh random morphology. Therefore, some modifications in the experimental design should be considered in future works. The fluid flow should be extensively studied, as there are scarce literature references using nanofiber meshes in perfusion bioreactors. In doing this, we will try to improve the ECM deposition. Additionally, as one of the factors that may also be influencing the results is the random morphology of the nanofiber meshes, different production techniques may be studied to obtain fully controlled morphologies.

Acknowledgment. M. Alves da Silva would like to acknowledge the Portuguese Foundation for Science and Technology (FCT) for her grant (SFRH/BD/28708/2006). The authors would like to acknowledge the patients of Hospital de S. Marcos, Braga, Portugal, for the donation of the biological samples, as well to its medical staff. The authors would also like to thank the Institute for Health and Life Sciences (ICVS), University of Minho, Braga, Portugal, for allowing the use of their research facilities. Authors would like specially to acknowledge Luis Martins for his valuable help with the histological procedures and Goreti Pinto for the aid in the microscopy. We thank Ana M. Frias for the important help with the FACS procedure. Finally, we would like to acknowledge the European NoE EXPERTISSUES (NMP3-CT-2004-500283). This work was partially supported by the European FP7 Project Find and Bind (NMP4-SL-2009-229292).

References and Notes

(1) Zhang, L.; Webster, T. J. *Nano Today* **2009**, 66–80.
(2) Chew, S. Y.; Wen, Y.; Dzenis, Y.; Leong, K. W. *Curr. Pharm. Des.* **2006**, *12*, 4751–70.
(3) Teo, W. E.; He, W.; Ramakrishna, S. *Biotechnol. J.* **2006**, *1*, 918–29.
(4) Huang, Z.-M.; Zhang, Y.-Z.; Kotaki, M.; Ramakrishna, S. *Compos. Sci. Technol.* **2003**, *63*, 2223–2253.
(5) Martins, A.; Chung, S.; Pedro, A. J.; Sousa, R. A.; Marques, A. P.; Reis, R. L.; Neves, N. M. *J. Tissue Eng. Regen. Med.* **2009**, *3*, 37–42.
(6) Thorvaldsson, A.; Stenhamre, H.; Gatenholm, P.; Walkenstrom, P. *Biomacromolecules* **2008**, *9*, 1044–9.
(7) Venugopal, J.; Low, S.; Choon, A. T.; Ramakrishna, S. *J. Biomed. Mater. Res., Part B* **2008**, *84*, 34–48.
(8) Pham, Q. P.; Sharma, U.; Mikos, A. G. *Biomacromolecules* **2006**, *7*, 2796–805.
(9) Park, J. S.; Park, K.; Woo, D. G.; Yang, H. N.; Chung, H. M.; Park, K. H. *Biomacromolecules* **2008**, *9*, 2162–9.
(10) Pinho, E. D.; Martins, A.; Araujo, J. V.; Reis, R. L.; Neves, N. M. *Acta Biomater.* **2009**, *5*, 1104–14.
(11) Alves da Silva, M. L.; Crawford, A.; Mundy, J. M.; Martins, A.; Araujo, J. V.; Hatton, P. V.; Reis, R. L.; Neves, N. *Tissue Eng.* **2009**, *15*, 377–385.
(12) Chung, C.; Burdick, J. A. *Adv. Drug Delivery Rev.* **2008**, *60*, 243–62.
(13) Vasita, R.; Katti, D. S. *Int. J. Nanomed.* **2006**, *1*, 15–30.
(14) Wang, Y.; Blasioli, D. J.; Kim, H. J.; Kim, H. S.; Kaplan, D. L. *Biomaterials* **2006**, *27*, 4434–42.
(15) DeLise, A. M.; Fischer, L.; Tuan, R. S. *Osteoarthritis Cartilage* **2000**, *8*, 309–34.
(16) Seda Tigli, R.; Ghosh, S.; Laha, M. M.; Shevde, N. K.; Daheron, L.; Gimble, J.; Gumusderelioglu, M.; Kaplan, D. L. *J. Tissue Eng. Regener. Med.* **2009**, *3*, 348–360.
(17) Loken, S.; Jakobsen, R. B.; Aroen, A.; Heir, S.; Shahdadfar, A.; Brinchmann, J. E.; Engebretsen, L.; Reinholt, F. P. *Knee Surg. Sports Traumatol. Arthrosc.* **2008**, *16*, 896–903.
(18) Lee, R. H.; Kim, B.; Choi, S.; Kim, H.; Choi, H. S.; Suh, K.; Bae, Y. C.; Jung, J. S. *Cell. Physiol. Biochem.* **2004**, *14*, 311–324.
(19) Teramura, T.; Fukuda, K.; Kurashimo, S.; Hosoi, Y.; Miki, Y.; Asada, S.; Hamanishi, C. *BMC Musculoskeletal Disord.* **2008**, *9*, 86.
(20) Janjanin, S.; Li, W. J.; Morgan, M. T.; Shanti, R. M.; Tuan, R. S. *J. Surg. Res.* **2008**, *149*, 47–56.
(21) Mahmoudifar, N.; Doran, P. M. *Biomaterials* **2005**, *26*, 7012–7024.
(22) Martin, I.; Miot, S.; Barbero, A.; Jakob, M.; Wendt, D. *J. Biomech.* **2007**, *40*, 750–65.
(23) Darling, E. M.; Athanasiou, K. *Tissue Eng.* **2003**, *9*, 9–26.
(24) Costa, P.; Martins, A.; Gomes, M.; Neves, N. M.; Reis, R. L. European PatentEP 2151491 A2, 2010, p 11.
(25) Guimarães, A.; Martins, A.; Pinho, E. D.; Faria, S.; Reis, R. L.; Neves, N. M. *Nanomedicine (London)* , *5*, 539–54.
(26) http://frodo.wi.mit.edu/.
(27) Mahmoudifar, N.; Doran, P. M. *Tissue Eng.* 2006.
(28) Devarapalli, M.; Lawrence, B. J.; Madihally, S. V. *Biotechnol. Bioeng.* **2009**, *103*, 1003–15.
(29) Lawrence, B. J.; Devarapalli, M.; Madihally, S. V. *Biotechnol. Bioeng.* **2009**, *102*, 935–47.
(30) Sailon, A. M.; Allori, A. C.; Davidson, E. H.; Reformat, D. D.; Allen, R. J.; Warren, S. M. *J. Biomed. Biotechnol.* **2009**, *2009*, 873816.

(31) Aulin, C.; Foroughi, F.; Brown, R.; Hilborn, J. *J. Tissue Eng. Regener. Med.* **2009**, *3*, 188–95.
(32) Pazzano, D.; Mercier, K. A.; Moran, J. M.; Fong, S. S.; DiBiasio, D. D.; Rulfs, J. X.; Kohles, S. S.; Bonassar, L. J. *Biotechnol. Prog.* **2000**, *16*, 893–6.
(33) Davisson, T.; Sah, R. L.; Ratcliffe, A. *Tissue Eng.* **2002**, *8*, 807–16.
(34) Freed, L. E.; Hollander, A. P.; Martin, I.; Barry, J. R.; Langer, R.; Vunjak-Novakovic, G. *Exp. Cell Res.* **1998**, *240*, 58–65.
(35) Freyria, A. M.; Cortial, D.; Ronziere, M. C.; Guerret, S.; Herbage, D. *Biomaterials* **2004**, *25*, 687–97.
(36) Vunjak-Novakovic, G.; Martin, I.; Obradovic, B.; Treppo, S.; Grodzinsky, A. J.; Langer, R.; Freed, L. E. *J. Orthop. Res.* **1999**, *17*, 130–8.
(37) Butler, D. L.; Goldstein, S. A.; Guldberg, R. E.; Guo, X. E.; Kamm, R.; Laurencin, C. T.; McIntire, L. V.; Mow, V. C.; Nerem, R. M.; Sah, R. L.; Soslowsky, L. J.; Spilker, R. L.; Tranquillo, R. T. *Tissue Eng., Part B* **2009**, *15*, 477–84.
(38) Godara, P.; McFarland, C. D.; Nordon, R. E. *J. Chem. Technol. Biotechnol.* **2008**, *83*, 408–420.
(39) Porter, B.; Zauel, R.; Stockman, H.; Guldberg, R.; Fyhrie, D. *J. Biomech.* **2005**, *38*, 543–9.
(40) Mahmoudifar, N.; Doran, P. M. *Biomaterials* **2010**, *31*, 3858–67.
(41) Tarng, Y. W.; Casper, M. E.; Fitzsimmons, J. S.; Stone, J. J.; Bekkers, J.; An, K. N.; Su, F. C.; O'Driscoll, S. W.; Reinholz, G. G. *J. Biomed. Mater. Res., Part A* **2010**, *95*, 156–63.
(42) Johnstone, B.; Hering, T. M.; Caplan, A. I.; Goldberg, V. M.; Yoo, J. U. *Exp. Cell Res.* **1998**, *238*, 265–272.
(43) Indrawattana, N.; Chen, G.; Tadokoro, M.; Shann, L. H.; Ohgushi, H.; Tateishi, T.; Tanaka, J.; Bunyaratvej, A. *Biochem. Biophys. Res. Commun.* **2004**, *320*, 914–919.
(44) Tigli, R. S.; Gumusderelioglu, M. *Biotechnol. Bioeng.* **2009**, *104*, 601–10.
(45) Jung, Y.; Kim, S. H.; Kim, S. H.; Kim, Y. H.; Xie, J.; Matsuda, T.; Min, B. G. *J. Biomater. Sci., Polym. Ed.* **2008**, *19*, 61–74.
(46) Li, W. J.; Jiang, Y. J.; Tuan, R. S. *Tissue Eng., Part A* **2008**, *14*, 639–48.

BM100476R